

## 氧化石墨烯对红细胞功能的影响

吕祎彤<sup>1</sup>, 陈博友<sup>1,3</sup>, 陈佳林<sup>1</sup>, 董益阳<sup>1</sup>, 刘佳蕙<sup>2</sup>, 许立达<sup>1</sup>

1 北京化工大学 生命科学与技术学院, 北京 100029

2 北京大学 化学与分子工程学院分析测试中心, 北京 100871

3 中化石油营销有限公司, 北京 100031

吕祎彤, 陈博友, 陈佳林, 等. 氧化石墨烯对红细胞功能的影响. 生物工程学报, 2021, 37(11): 4047-4055.

Lv YT, Chen BY, Chen JL, et al. Effect of graphene oxide on the function of erythrocytes. Chin J Biotech, 2021, 37(11): 4047-4055.

**摘要:** 纳米材料的生物相容性是人们关注的热点。氧化石墨烯是一种被广泛应用于生物医学的纳米材料, 但其毒性不容忽视。本文从溶血率、红细胞脆性、乙酰胆碱酯酶活性三方面研究了氧化石墨烯对血液系统的毒性。结果表明, 红细胞的溶血率在氧化石墨烯浓度低于 100  $\mu\text{g}/\text{mL}$  时均低于 8% ( $P < 0.01$ ); 低浓度氧化石墨烯 ( $< 5 \mu\text{g}/\text{mL}$ ) 对红细胞的脆性没有显著影响, 高浓度氧化石墨烯 (如 10  $\mu\text{g}/\text{mL}$ ) 会提高红细胞的脆性 ( $P = 0.01$ ); 氧化石墨烯能增加红细胞上乙酰胆碱酯酶的活性, 浓度为 20  $\mu\text{g}/\text{mL}$  的直径  $> 5 \mu\text{m}$  的氧化石墨烯 (LGO) 可将乙酰胆碱酯酶的活性提高 42.67% ( $P < 0.05$ )。之后利用分子动力学模拟研究氧化石墨烯与乙酰胆碱酯酶相互作用并提高其活性的机理, 推测氧化石墨烯会附着在细胞膜上并提供一个电负性环境, 帮助水解产物更快地从活性位点脱离, 从而提高乙酰胆碱酯酶的活性。

**关键词:** 氧化石墨烯, 红细胞, 乙酰胆碱酯酶, 溶血率, 分子动力学模拟

## Effect of graphene oxide on the function of erythrocytes

Yitong Lv<sup>1</sup>, Boyou Chen<sup>1,3</sup>, Jialin Chen<sup>1</sup>, Yiyang Dong<sup>1</sup>, Jia-Hui Liu<sup>2</sup>, and Lida Xu<sup>1</sup>

1 College of Life Science and Technology, Beijing University of Chemical Technology, Beijing 100029, China

2 Analytical Instrumentation Center, College of Chemistry and Molecular Engineering, Peking University, Beijing 100871, China

3 Sinochem Oil Marketing Co., Ltd., Beijing 100031, China

**Abstract:** The biocompatibility of nanomaterials has attracted much attention. Graphene oxide (GO) is a nanomaterial widely used in biomedicine, but its toxicity can not be ignored. In this study, the effect of GO on the blood system (the hemolysis rate, the fragility of erythrocyte, and acetylcholinesterase activity) was systematically investigated. The results showed that the hemolysis rate of erythrocytes was lower than 8% when the GO concentration was below 100  $\mu\text{g}/\text{mL}$  ( $P < 0.01$ ).

**Received:** December 16, 2020; **Accepted:** March 28, 2021

**Supported by:** National Mega-project for Innovative Drugs (No. 2019ZX09721001-007-002), Joint Project of BRC-BC (Biomedical Translational Engineering Research Center of BUCT-CJFH), China (No. RZ2020-02).

**Corresponding authors:** Jia-Hui Liu. Tel: +86-10-62754181; E-mail: jhliu@pku.edu.cn

Lida Xu. Tel: +86-10-64421335; E-mail: xuld@mail.buct.edu.cn

国家十三五科技重大专项 (No. 2019ZX09721001-007-002), 北京化工大学-中日友好医院生物医学转化工程研究中心项目 (RZ2020-02) 资助。

网络出版时间: 2021-05-06

网络出版地址: <https://kns.cnki.net/kcms/detail/11.1998.q.20210430.1700.003.html>

GO at low concentration levels ( $<5 \mu\text{g/mL}$ ) had no significant effect on the fragility of erythrocytes, but GO at high concentration ( $10 \mu\text{g/mL}$ ) increased the fragility of erythrocytes ( $P=0.01$ ). Moreover, GO increased the activity of acetylcholinesterase on erythrocytes. The concentration of  $20 \mu\text{g/mL}$  graphene oxide with the size  $>5 \mu\text{m}$  (LGO) increased the activity of acetylcholinesterase by 42.67% ( $P<0.05$ ). Then molecular dynamics simulation was used to study how GO interacted with acetylcholinesterase and increased its activity. The results showed that GO was attached to the cell membrane, thus may provide an electronegative environment that helps the hydrolysate to detach from the active sites more quickly so as to enhance the activity of acetylcholinesterase.

**Keywords:** graphite oxide, erythrocyte, acetylcholinesterase, hemolysis rate, molecular dynamics simulation

## Introduction

Due to the excellent biocompatibility and large surface area, nanomaterials are often employed in efficient drug delivery systems<sup>[1-2]</sup>. In the last decade, graphene-family nanomaterials, particularly graphene oxide (GO) and graphene, have been used as novel nanocarriers for therapeutic diagnostics due to their potentials to reduce multi-drug resistance and non-specific targeting<sup>[3]</sup>. Especially, GO showed better adsorption stability and biocompatibility than graphene as reported by Yu et al<sup>[4]</sup>. Moreover, Chen et al<sup>[5]</sup> found that 1–10 mg/mL GO could increase the activity of acetylcholinesterase.

The toxicity of GO is an important factor in determining its applications. GO may interfere with the normal physiological function of vital organs, leading to acute inflammatory responses and chronic injury<sup>[6]</sup>. Lv et al<sup>[7]</sup> found that the viability of human neuroblastoma SH-SY5Y cells decreased to 20% after treatment with 100 mg/mL GO for 96 h. Meanwhile, some studies have shown that the toxicity of GO can be reduced under some conditions. Hu et al<sup>[8]</sup> reported that GO showed concentration-dependent cytotoxicity, which was greatly alleviated at the 10% fetal bovine serum (FBS) concentration commonly used in cell culture media, due to the high protein adsorption capacity of GO.

Since drug carriers may distribute in the body through the blood system, the effects of GO on the blood system is worthy to be discussed. Red blood cells (RBCs) were often used to evaluate the hemocompatibility of biomedical materials. But the toxicity of GO to RBCs is unclear. Some studies<sup>[9-10]</sup> have found that the GO had effects on RBCs morphology, and the toxicity of GO was environment-dependent. However, some studies have shown<sup>[11-13]</sup> that GO did not cause significant

hemolysis of RBCs at some concentrations and conditions. To further evaluate the effect of GO on the properties of RBCs, we studied their interactions through hemolysis experiments and fragility experiments.

In addition to the effects of GO on the cell morphology, the effect on cellular function is also an important aspect. Membrane proteins are important components for cellular functions, since they can maintain the membrane stability and signal transductions. The changes in membrane protein activity can reflect the effects of GO on cellular functions. Acetylcholinesterase (AChE) is an important enzyme located on the erythrocyte membrane, which plays an important role in maintaining the morphology of RBCs. The change of AChE activity has been reported to affect the efficiency of the oxygen transport of RBCs, and also affect the pathological conditions of human bodies<sup>[14-16]</sup>. Here, the AChE activities under GO exposure was studied, and the mechanism of GO on AChE was further studied through simulation methods.

## 1 Materials and methods

### 1.1 Hemolysis assay

The blood was taken from ICR mice and used heparin sodium as an anticoagulant. Typically, 1 mL of whole blood was added to 5 mL of phosphate-buffered saline and centrifuged at 2500 r/min for 5 min to isolate RBCs from serum. This purification step was repeated three times, and then the washed RBCs were diluted to 50 mL in phosphate-buffered saline. To test the hemolytic activity of two kinds of GOs, 0.9 mL diluted RBCs suspension was taken out and mixed with 0.1 mL of GO solution in phosphate-buffered saline at systematically varied concentrations (1, 5, 10, 20, 50, 100  $\mu\text{g/mL}$ ). The

GO solutions of different levels were prepared immediately before the dilution of the RBCs. For negative control samples, 0.9 mL of RBCs suspension was mixed with 0.1 mL phosphate-buffered saline and water, respectively. For positive control samples, 0.9 mL Triton X-100 was mixed with 0.1 mL of phosphate-buffered saline. Then, all the samples were incubated in a humidified incubator at 37 °C, 5% CO<sub>2</sub> for 1 h, and centrifuged at 2 500 r/min for 5 min. 200 μL of the supernatant of all the samples were added to coated wells separately, measured by the enzyme-labelled instrument. The following formula was used to calculate the RBCs hemolysis:  $\text{hemolysis}\% = (\text{sample absorbance} - \text{negative control absorbance}) / (\text{positive control absorbance} - \text{negative control absorbance}) \times 100\%$ .

## 1.2 Effect of RBCs on the morphology

### 1.2.1 RBCs morphology

GO of two different sizes were added to the RBC samples respectively. Next, the cell suspension was inhaled into the syringe, and a micro-sieve filter was applied to filter the free cells to attach to the inlet microporous membrane. Took out the filter membrane and fold it in half twice, put it into the dehydration basket for ethanol dehydrate. Tert-butanol was used for 1:1 replacement with anhydrous ethanol for two times, the third addition of tert-butanol just over the basket, and finally put samples in the refrigerator to freeze. After freezing, the mechanical vacuum pump was used to vacuum for 2 hours. The sample was dried in vacuo to obtain a powder sample, fixed in the scanning electron microscope (SEM) sample stage, and then the gold coating was used to observe the cell morphology.

### 1.2.2 Fragility of RBCs

The blood was washed with phosphate-buffered saline (PBS) three times. RBCs samples containing 0, 5, 10, 20, 50, and 100 μg/mL GO were incubated at 37 °C for 30 min and washed three times, then fixed with 2% glutaraldehyde for 30 min and washed by 0.1 mol/L PBS buffer three times. NaCl of 0.4%, 0.5%, 0.6% were prepared to provide environment with different osmotic pressures. 40 μL of samples were added to different concentrations of NaCl. After standing at room temperature for 10 min, the samples were centrifuged at 2 000 r/min

for 3 min. 200 μL supernatant were added to a 96-well plate and measured at 450 nm absorbance using a microtiterplate reader. The calculation formula of hemolysis rate is the same as 1.1.

### 1.3 AchE activity estimation

AchE catalyzes the hydrolysis of the substrate acetylcholine into acetic acid and thiocholine, which uses 5,5'-dithiobis (2-nitrobenzoic acid) (DTNB) to yield 5-thio-2-nitrobenzoic acid. Because 5-thio-2-nitrobenzoic acid has a maximum absorption at 412 nm, its amount per unit time was measured to calculate the activity of AchE. The blood was diluted to 15 mL using culture medium (1640, 5% FBS, 1% double-antibody), then 1 mL RBCs diluent was added to the six-well plate and diluted to 3 mL. GO with different diameters at 0, 1, 5, 10, 15, and 20 μg/mL were added to the RBCs diluent and cultured for one day. RBCs diluent was centrifuged to wash away the GO, resuspended to 3 mL. Two different GO dispersants were designed in this experiment, one was deionized water, and the other was 0.5% BSA. After that, added 1 mL substrate, placed in 37 °C water bath for 60 min. The sample was centrifuged at 1 500 r/min for 5 min, 3 mL of the supernatant was aspirated, and the color was developed by adding 10 μL of hydrochloric acid and 200 μL of DTNB. The absorbance of each sample was measured at 405 nm. Using the following formula to calculate the AchE activity:  $\text{activity}\% = (\text{sample absorbance} - \text{negative control absorbance}) / (\text{positive control absorbance} - \text{negative control absorbance}) \times 100\%$ .

### 1.4 Molecular dynamics simulations

To understand the process how GO contacted with the cell membrane and protein, simulations of GO with free AchE and with AchE on membrane were performed. Atomistic MD simulations were performed using Gromacs 2018.1 with the CHARMM36 force field. The 3D structure of AchE was obtained from the Protein Data Bank with PDB entry code 2JGM. The dipalmitoyl phosphatidyl choline (DPPC) bilayer is constructed by CHARMM-GUI. The system energy was minimized using the conjugate gradient method. The water was defined by the TIP3 model. The time step of each atomistic MD simulation was set as 2 fs. For each

simulation, the GO and AchE were inserted with 60 Å distance between their center of mass at the beginning, which made sure that the simulation results were not affected by the van der Waals force and the electrostatic interactions. The simulation lasted 30 ns and was repeated three times. GROMACS 2018.1 software<sup>[17]</sup> was used as an important tool for trajectory analyses. All visualization and graphics were prepared using VMD.

## 2 Results

### 2.1 Characterization of GO

GOs with the sizes of <500 nm and >5 μm were purchased from XFNANO. The dimensions of GOs had been confirmed by atomic force microscopy

(AFM-Multimode-8) (Fig. 1). According to the scale, the two sizes of GOs were referred as SGO and LGO, respectively. Although the GOs had different sizes, they both retained the lamellar structure with a thickness of 2–3 nm.

The zeta potential is usually an indicator of the stability of the system. When the zeta potential is between  $\{-5,5\}$ , the particles in the solution are highly agglomerated. When the zeta potential exceeds  $\pm 60$ , the particles have excellent durability. As shown in Fig. 2, the zeta potential of GO dispersed by deionized water was  $-30$  mV and  $-31$  mV, and the zeta potential of GO dispersed by bovine serum albumin (BSA) were  $-10$  mV and  $-8$  mV. The results proved that both sizes of GO had good stabilities.

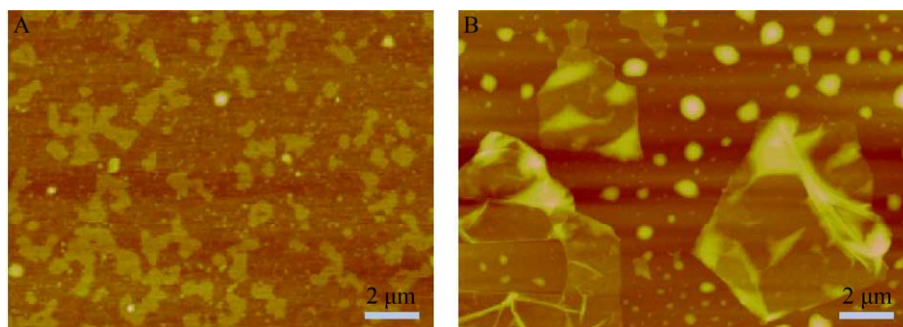


图1 直径< 500 nm (A) 和直径> 5 μm (B) 氧化石墨烯的 AFM 表征图

Fig. 1 AFM image for different size of GO. (A) SGO with the size<500 nm. (B) LGO with the size>5 μm.

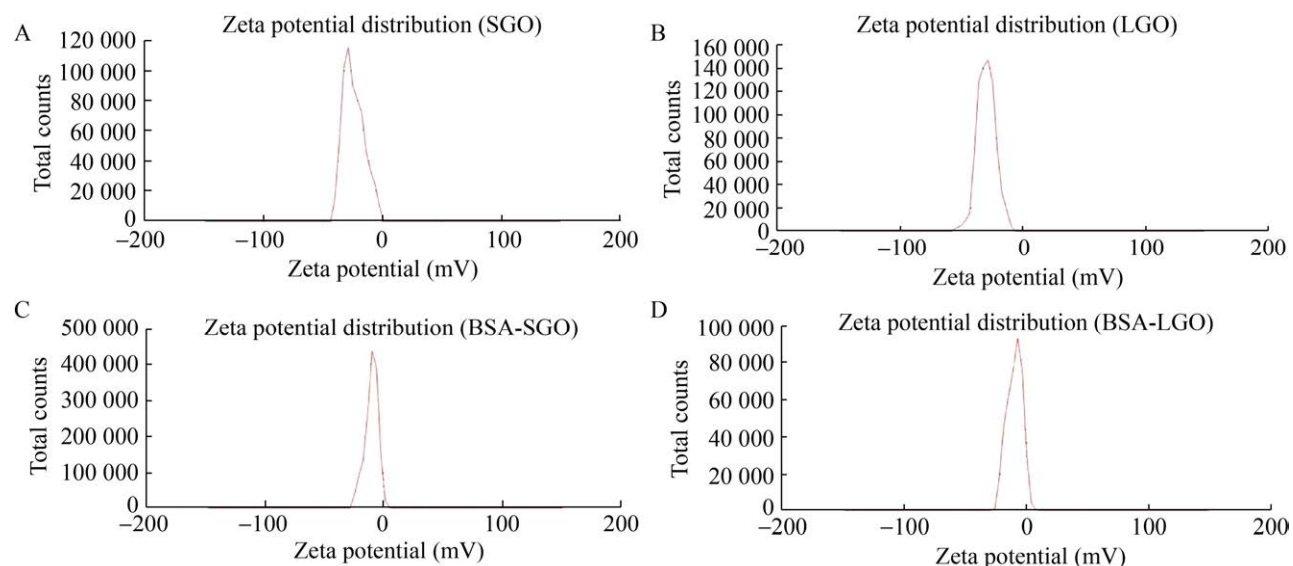


图2 SGO 和 LGO 在 NaCl 溶液 (A–B) 和牛血清蛋白 (C–D) 中的 Zeta 电位

Fig. 2 The zeta potential of GO, in NaCl solution (A–B) and in bovine serum albumin (C–D).

As shown in Fig. 3, the contents of C and O were determined by XPS method. The content of O in LGO was 31.04 wt%, which was significantly higher than 24.86 wt% in SGO. The contents of C in SGO (52.47 wt%) and LGO (51.69 wt%) were not much different. The results of XPS showed that the number of oxygen-containing functional groups in SGO and LGO were different, which may lead to their different functions.

## 2.2 Effect of GO on the morphology of the RBCs

When RBCs were co-incubated with 20  $\mu\text{g/mL}$  GO at the two different sizes, the morphology of RBCs was not significantly affected and retained vesicles. The morphology of the RBCs co-incubated with SGO was nearly not changed, while a small portion of the RBCs co-incubated with LGO was destroyed (Fig. 4A–C).

The amount of haemoglobin released from RBCs is an indicator of cell damage after contacting with GO. In the hemolysis test, the hemolysis rate of RBCs did not change significantly with the increase of LGO concentration. The hemolysis rate caused by adding SGO was a little higher than that caused by adding LGO, but still less than 8% (Fig. 5A). Therefore, it could be considered that LGO had no significant effect on RBCs' morphology at less than 100  $\mu\text{g/mL}$ , while SGO increased the hemolysis rate of RBCs ( $t$ -test:  $P < 0.01$ ).

Fragility test is an experiment where hemolysis changes are measured when decreasing the osmotic pressure. The fewer percentage of RBCs fractured, the tougher the system was. Since SGO and LGO

have a similar effect on the hemolysis of RBCs while the concentration of GO changing, SGO was chosen as a representative for further fragility test. According to the experimental data, the hemolysis rate changed sharply when NaCl concentration increased from 0.4% to 0.6% (Fig. 5B). Then, the hemolysis rates were examined in 0.4%, 0.5% and 0.6% NaCl solutions. As shown in Fig. 5C, when the concentration of NaCl was 0.6%, the hemolysis rates increased from 18.64% to 30.45% with the concentration of GO ranging from 0 to 10  $\mu\text{g/mL}$ , which were much lower than the hemolytic rates in the condition of 0.5% or 0.4% NaCl solution. The fragility of RBC was not significantly changed with GO at low concentrations (less than 5  $\mu\text{g/mL}$ ); when the concentration of GO was at 10  $\mu\text{g/mL}$ , the RBC fragility was significantly raised (two-way variance analysis:  $P = 0.01$ ), and the average hemolysis rate was increased to 77.95% in the condition of 0.5% NaCl concentration.

## 2.3 AchE activity estimation

The changes of AchE activity can reflect the effect of GO on the cell function of RBCs. As shown in Fig. 6, the addition of SGO and LGO increased the activity of AchE, especially LGO increased the activity by 42.67%. That were probably related to the number of oxygen-containing functional groups within them, which may attract the substrates by forming hydrogen bonds with the carbonyl oxygen of the substrate. However, in the dispersed solution of BSA, the activity of AchE changed little. GO is electrically negative due to its own oxygen-containing energy

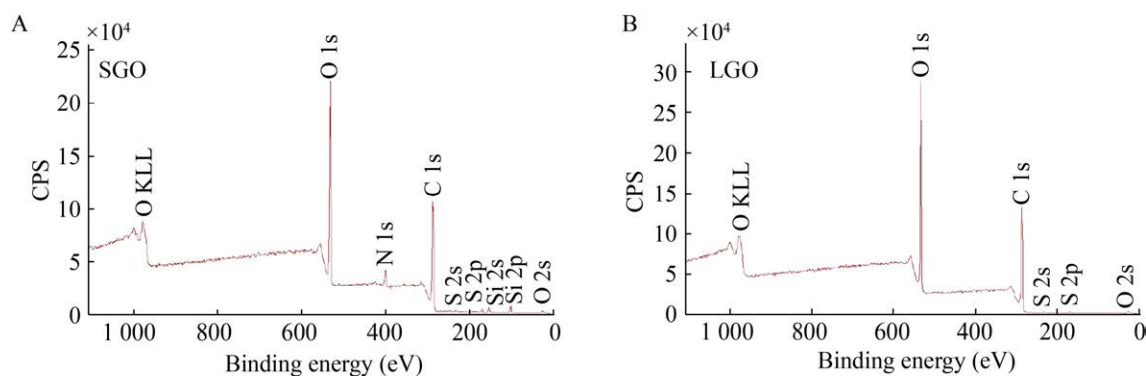


图3 SGO (A) 和 LGO (B) 的 XPS 表征结果

Fig. 3 The XPS result of SGO (A) and LGO (B).

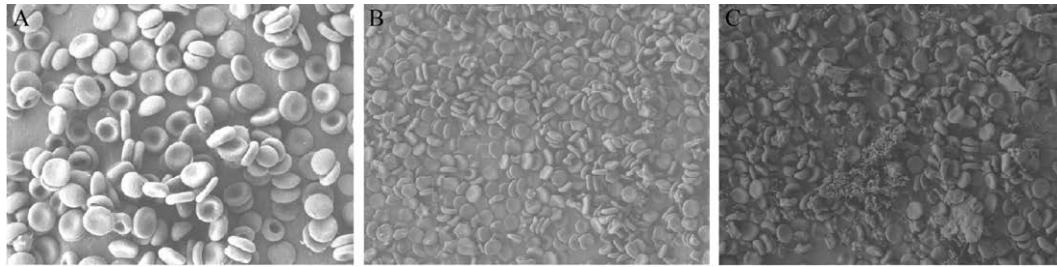


图 4 无 GO (A) 和与 SGO (B) 或 LGO (C) 共培养时红细胞的 SEM 表征图

Fig. 4 SEM results of RBCs incubated without GO (A) and with SGO (B) or LGO (C).

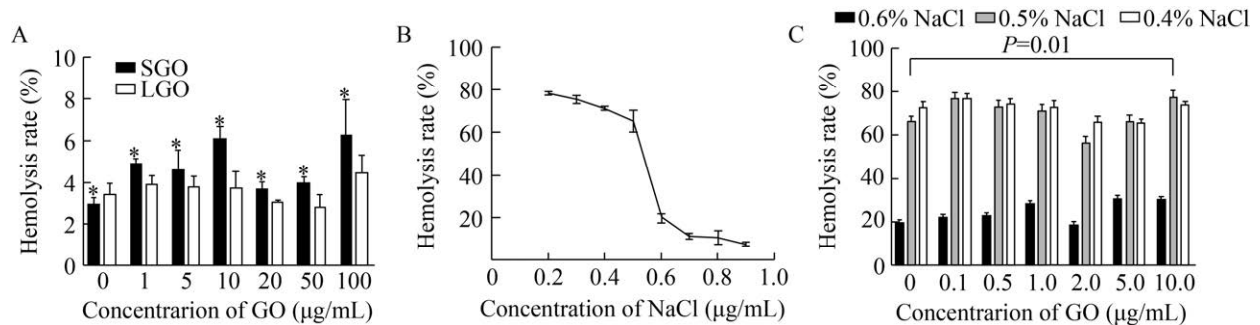


图 5 红细胞的溶血率变化 (A: NaCl 溶液中红细胞与 SGO 或 LGO 共培养时的溶血率 ( $P < 0.05$ ), B: 红细胞溶血率随渗透压的变化曲线, C: 与不同浓度 LGO (SGO) 共培养的红细胞在 0.4%, 0.5% 或 0.6% NaCl 溶液中的溶血率)

Fig. 5 Changes in hemolysis rate of red blood cells. (A) Hemolysis rate of RBCs incubated with SGO or LGO in NaCl ( $P < 0.05$ ). (B) The curve of hemolysis rate of RBCs with osmotic pressure. (C) Hemolysis rate of RBC incubated with different concentrations of LGO (SGO) in 0.4%, 0.5% or 0.6% NaCl solution.

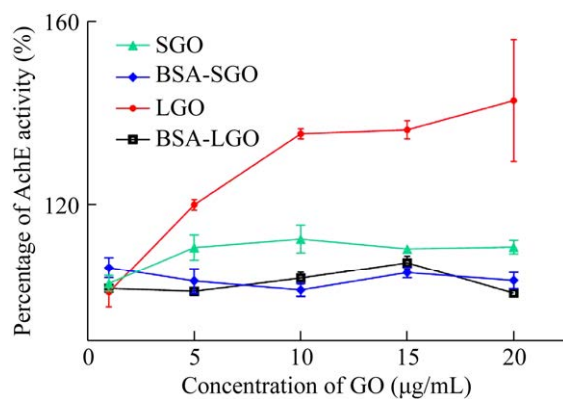


图 6 乙酰胆碱酯酶的活性变化 ( $P < 0.05$ )

Fig. 6 The activities of acetylcholinesterase on RBCs changed with the concentrations of SGO or LGO in NaCl solution or bovine serum albumin ( $P < 0.05$ ).

group. The electronegativity of GO was reduced in BSA solution. Thus, it could be seen that changes in the electrical properties of GO had effects on the activity of AchE.

## 2.4 Molecular dynamic simulations

In previous studies, the AchE activity of free-state was decreased in the presence of GO<sup>[18]</sup>. To investigate how the cell membrane environment affected the activity of AchE with GO, the molecular dynamic simulations were used to study the interaction between GO and AchE in the membrane environment. In order to further explore the difference in the effects of GO on AchE activity within and without the membrane environment, these two systems were simulated and compared. The active sites of AchE were composed of several different residues, including Tyr72, Tyr124, Ser203, Trp236, Tyr286, Phe295, Phe297, Glu334, Tyr337, Phe338, Tyr341 and His447. The opening of active sites is essential for the maintenance of enzyme activity. After simulated for 30 ns, GO was gradually absorbed onto the surface of AchE and blocked part of the active sites in the system of GO with free-AchE (Fig. 7A–B). However, for the system

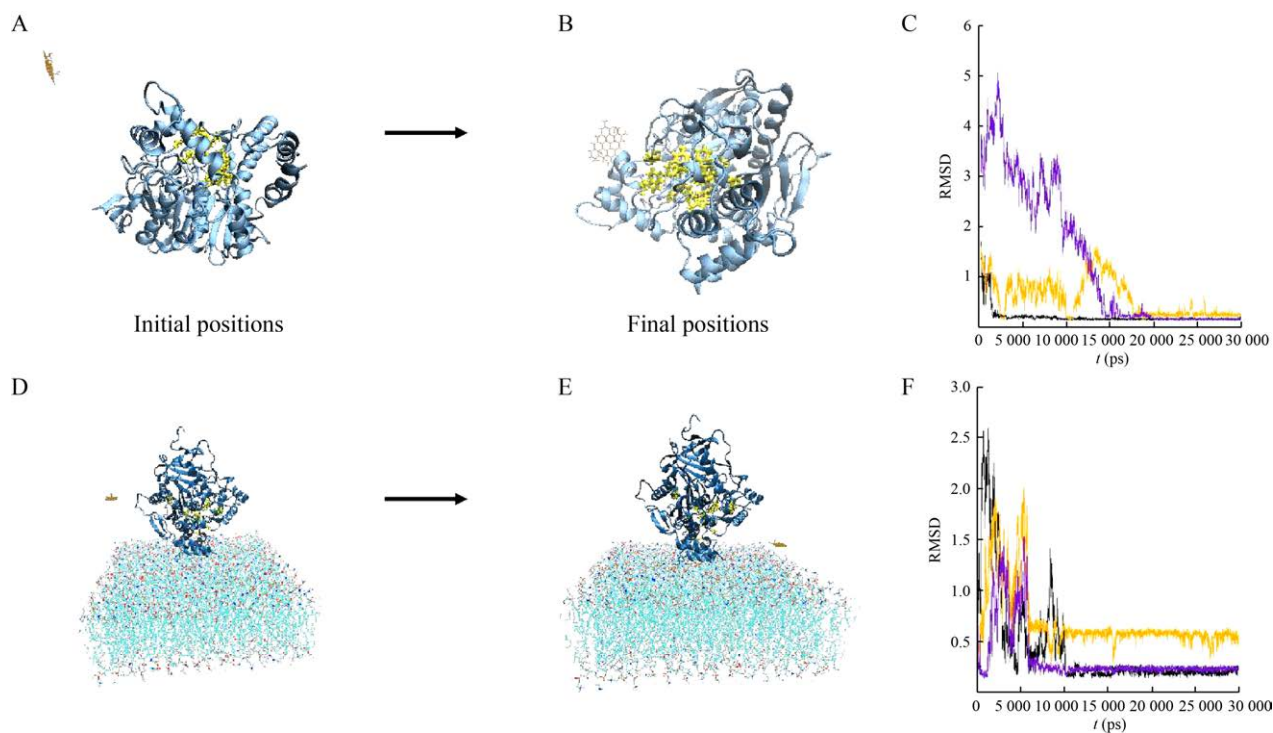


图7 氧化石墨烯和乙酰胆碱酯酶在无膜环境 (A–C) 和有膜环境 (D–F) 中的模拟结果. (氧化石墨烯为棕色, 乙酰胆碱酯酶为蓝色, 乙酰胆碱酯酶的活性位点用黄色表示. RMSD 曲线表明两个体系均已达到平衡 (C, F))  
 Fig. 7 The interactions of GO with free AchE (A–C) and with AchE on membrane (D–F) in the simulations. The GO is brown. The AchE is blue. The active sites on AchE are yellow. RMSD results show that both systems are in equilibrium (C, F).

in membrane environment, the distance between GO and the membrane was decreasing, and the active sites of AchE maintained exposed during the simulations (Fig. 7D–E). The curves in Fig. 7C and Fig. 7F, which represent the root-mean-squared deviation (RMSD) changes in three independent simulation processes for each system, tended to be stable after a period of simulation time, indicating that the simulated systems had reached equilibrium states.

### 3 Discussion

Understanding the toxicity of nanomaterials is very important for their applications. Taking advantage of the unique properties of nanomaterials and avoiding their toxicity will further increase the application range of nanomaterials. In this study, the effects of GO on RBCs were systematically evaluated. As shown in the above results, GOs at the size of <math><500\text{ nm}</math> and <math>>5\text{ }\mu\text{m}</math> have similar effects on

RBCs. Generally, their effects on RBC morphology and hemolytic properties were not significant. In particular, the hemolysis experiments showed that the two sizes of GOs did not cause significant hemolysis at GO concentrations less than  $100\text{ }\mu\text{g/mL}$ . Fragility tests showed that the addition of GO had some effects on the hemolytic rate of RBCs at different NaCl concentration.

The impact of nanomaterials on the function of the RBCs can be partially evaluated by monitoring the activities of membrane proteins on RBCs, since the membrane proteins mediate important functions such as signal transmission. The reason why GO affects the enzyme activity may be that the functional group of GO forms hydrogen bonds with the carbonyl oxygen of the substrate, which enriches the substrate around GO. At the same time, the negatively charged GO keeps the carboxylic acid of the decomposition product of the substrate away from the enzyme through charge repulsion,

thereby increasing the activity of the enzyme. Our experiments showed that LGO has a greater impact on enzyme activity in NaCl solution. This may be due to the different oxygen content of LGO and SGO, which results in different numbers of oxygen-containing functional groups. However, LGO and SGO dispersed in BSA solution had little difference on enzyme activity. This could be due to that the substrate gathered near the enzyme, and the electrically neutral environment could not make GO accelerate the carboxylic acid to leave the position of the enzyme through charge repulsion in BSA solution. Therefore, BSA-dispersed GO had little difference on enzyme activity. The addition of GO increased the activity of AchE on RBCs, while AchE activity in bovine serum albumin solution did not change significantly with the increase of GO. The reason may be that the membrane environment increases the electronegativity of GO in NaCl solution, accelerating the rate of carboxylic acid away from the enzyme. For BSA-dispersed GO, the solution remained electrically neutral, which had little impact on the enzyme activity. Meanwhile, it has been reported that the activity of free AchE decreases after co-incubated with GO. The key factor inducing the contrary effects is the membrane environment. Our simulation results showed that the interaction between GO and AchE was different within and without membrane environments. In a membrane-free environment, GO gathered around AchE, potentially blocking the active sites of AchE, while in the membrane environment, GO tends to adsorb on the cell membrane, avoiding obstructing the substrate binding to the active sites of AchE.

Based on the above experimental results, it can be concluded that the toxicity of GO on RBCs can be significantly decreased. GO would probably attach to or insert into the membrane of RBCs, causing a small amount of damage to the membrane, but reducing the hemolysis rate because of its aggregation, without affecting the adaptability of the RBCs to the hypotonic environment. At the same time, GO increases the electronegativity of the solution, making it easier for the substrate to gather around the membrane protein for interaction, and

can repel the carboxylic acid produced by the decomposition of the substrate in the membrane environment, so as to increase the membrane protein activities. The results suggest that GO has good biocompatibility with the blood system.

## Acknowledgements

Thank Dr. Jinglin Xie for the measurement of XPS performed at the Analytical Instrumentation Center of Peking University.

## REFERENCES

- [1] Hashemzadeh H, Raissi H. Understanding loading, diffusion and releasing of doxorubicin and paclitaxel dual delivery in graphene and graphene oxide carriers as highly efficient drug delivery systems. *Appl Surf Sci*, 2020, 500: 144220.
- [2] Han XM, Zheng KW, Wang RL, et al. Functionalization and optimization-strategy of graphene oxide-based nanomaterials for gene and drug delivery. *Am J Transl Res*, 2020, 12(5): 1515-1534.
- [3] Guo XQ, Mei N. Assessment of the toxic potential of graphene family nanomaterials. *J Food Drug Anal*, 2014, 22(1): 105-115.
- [4] Yu ZS, Gao YY, Wang XG, et al. Comparison of adsorption of proteins at different sizes on pristine graphene and graphene oxide. *Chin J Chem Phys*, 2018, 31(1): 10.1063.
- [5] Chen Z, Yu C, Khan IA, et al. Toxic effects of different-sized graphene oxide particles on zebrafish embryonic development. *Ecotoxicol Environ Saf*, 2020, 197: 110608.
- [6] Ou LL, Song B, Liang HM, et al. Toxicity of graphene-family nanoparticles: a general review of the origins and mechanisms. *Part Fibre Toxicol*, 2016, 13: 57.
- [7] Lv M, Zhang YJ, Liang L, et al. Effect of graphene oxide on undifferentiated and retinoic acid-differentiated SH-SY5Y cells line. *Nanoscale*, 2012, 4(13): 3861-3866.
- [8] Hu WB, Peng C, Lv M, et al. Protein corona-mediated mitigation of cytotoxicity of graphene oxide. *ACS Nano*, 2011, 5(5): 3693-3700.

- [9] Liao KH, Lin SY, Macosko CW, et al. Cytotoxicity of graphene oxide and graphene in human erythrocytes and skin fibroblasts. *ACS Appl. Mater. Interfaces*, 2011, 3(7): 2607-2615.
- [10] Feng R, Yu YP, Shen CX, et al. Impact of graphene oxide on the structure and function of important multiple blood components by a dose-dependent pattern. *J Biomed Mater Res Part A*, 2014, 103(6): 2006-2014.
- [11] Qu GB, Wang XY, Liu Q, et al. The *ex vivo* and *in vivo* biological performances of graphene oxide and the impact of surfactant on graphene oxide's biocompatibility. *J Environ Sci*, 2013, 25(5): 873-881.
- [12] Wang Y, Zhang BM, Zhai GX. The effect of incubation conditions on the hemolytic properties of unmodified graphene oxide with various concentrations. *RSC Adv*, 2016, 6(72): 68322-68334.
- [13] Kim HM, Kim KM, Lee K, et al. Nano-bio interaction between graphite oxide nanoparticles and human blood components. *Eur Chem Soc Publ*, 2012, 2012(32): 5343-5349.
- [14] Gupta S, Belle VS, Rajashekhar RK, et al. Correlation of red blood cell acetylcholinesterase enzyme activity with various RBC indices. *Ind J Clin Biochem*, 2018, 33(4): 445-449.
- [15] Bourne Y, Radic Z, Taylor P, et al. Conformational remodeling of femtomolar inhibitor-acetylcholinesterase complexes in the crystalline state. *J Am Chem Soc*, 2011, 132(51): 18292-18300.
- [16] Bourne Y, Sharpless KB, Taylor P, et al. Steric and dynamic parameters influencing *in situ* cycloadditions to form triazole inhibitors with crystalline acetylcholinesterase. *J Am Chem Soc*, 2016, 138(5): 1611-1621.
- [17] Abraham MJ, Murtola T, Schulz R, et al. GROMACS: high performance molecular simulations through multi-level parallelism from laptops to supercomputers. *SoftwareX*, 2015, 1-2(C): 19-25.
- [18] Wang Y, Gu Y, Ni YN, et al. Inhibition effect of graphene oxide on the catalytic activity of acetylcholinesterase enzyme. *Luminescence*, 2015, 30(7): 940-946.

(本文责编 郝丽芳)